

Design, Modeling and Performance Evaluation of a Long and Slim Continuum Robotic Cable

Manas M. Tonapi, Isuru S. Godage, and Ian D. Walker, *Fellow, IEEE*

Abstract— In this paper, we present a novel design for constructing multi-section continuum robots with a special focus on thin (less than 1 cm diameter) and relatively longer length (more than 100 cm), along with its new kinematic modeling and performance evaluation. This spring-loaded, tendon-actuated cable-like continuum robot incorporates key features of a concentric tube style design with added local compression to most sections and actively controllable bending along its entire backbone. It also avoids a complicated and large actuator system. Such robotic cables can be well suited for current space and terrestrial applications like exploration, teleoperation, surveillance, maintenance activities, etc., benefiting from these unique structural properties.

adversely [5]. The long and thin aspect ratio of “Tendril”-like robots could have prospective terrestrial and space applications in areas of defense and security, remote exploration, alternatives to certain applications in industrial automation, teleoperation in hazardous environmental conditions etc. Hence, there is a need for new and better designs. Until now, different kinds of continuum and continuum style snake and hyper redundant robotic manipulators [6-7] have been materialized. From the point of view of slender but long robotic cables, several of the existent designs have desirable functionalities. These robots are reviewed below with respect to their mechanical design and actuator system required.

Implementation of a thin, flexible continuum arm with an incompressible backbone is described in [8]. It was actuated

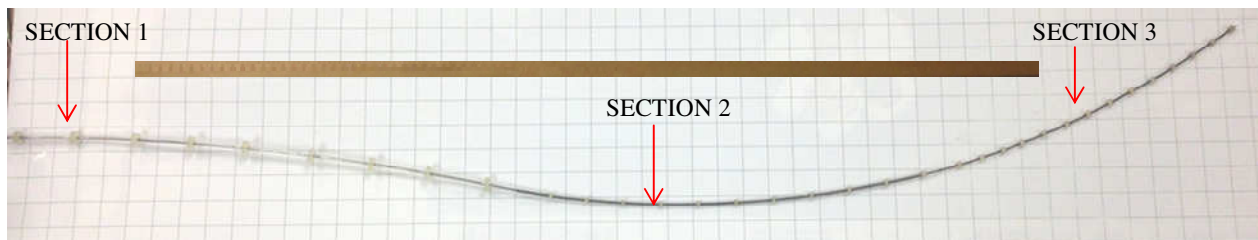


Figure 1. Long and slim continuum robotic cable (alongside a yardstick)

I. INTRODUCTION

Continuum robots are smooth, continuous structures which make use of elastic deformation allowing them to penetrate congested environments as well as perform grasping and manipulation in a unique way [1]. The majority of continuum robot designs have constant curvature sections and follow one of three major design philosophies viz., tendon-based approaches, concentric-tube designs and locally actuated backbone designs [2].

These continuous backbone robots are mostly broad in profile and relatively short in length. Design of thin but relatively short continuum robots has been seen in some medical applications involving Minimally Invasive Surgery (MIS) [3]. “Tendril” was the first generation long and thin continuum robot for inspection use in space [4]. However, its design has significant limitations affecting its performance

by tendons in such a way that bendable sections possessed approximately uniform torsion and curvature. Many other shapes were attained by changing section lengths in its variant design [9]. Both, however, lacked in achieving sectional compression/extension. Using shape memory alloys, a thin surgical snake robot was built [10], but had heating issues of the alloy and considerable mechanical complexity [11]. ShapeLock® technology [12] helps to achieve bending at arbitrary points along the length of a snake robot. An alternative implementation of this technology is seen in the highly articulated robotic probe (HARP) [11] and multi-turn catheter [13]. Both, however, have the disadvantage of substantially sized actuator system and significantly complex structural designs if a thin version is to be made.

Robots developed with a concentric tube structure [14] consisting of pre-curved tubes sliding within each other are commonly used in MIS. Some have restricted curving due to the pre bent nature of tubes but can achieve local extension and contraction as well as possessing a thin contour. A long continuum styled snake named active scope camera is seen in [7]. It can bend actively, specifically at the distal tip with the remaining body following suit. Like a snake, its motion is

*This research was supported in part by NASA under contract NNX12AM01G, and in part by the U.S. National Science Foundation under grant IIS-0904116.

M.M. Tonapi, I. S. Godage and I.D.Walker are with the Electrical & Computer Engineering Department, Clemson University, Clemson, SC 29634, USA (e-mail: {mtonapi, igodage, iwalker}@clemson.edu).

possible only in the presence of a contact surface. It also lacks the feature of local compression/extension.

Pneumatics or hydraulics [15-16] is the preferred actuation system implemented in continuum robots to achieve variable stiffness and/or in locally actuated backbone designs, since this enables the desired attribute of both limited local bending and extension. However, this comes at a cost of the requirement for a fluid/pressure regulatory system, which makes the design non-trivial with complex routing and valving arrangements and ultimately increases the size of the robot. Though better local steering is ensured by fixing motors within the backbone in robots like [17] the size is compromised making them bulky. An increase in length with such an approach will further complicate the design. In order to achieve the best of both worlds, snake and continuum elements have been mixed and matched to give hybrid robots [18]. However, since the influence of segmented backbones viz., snake structure, is predominant, this design becomes complicated and bulky.

The use of compression and extension springs in varied manifestations is prominent in different continuum robots. “Tendril” uses springs as backbone elements [4] to reduce its weight and make it slimmer. The surgical tool RAVEN uses a compliant probe made of compression springs to achieve bending by converting its ability of compressing and extending into bending, through tendons running on the inside of the spring [19]. A linearly actuated adapter provides the necessary translation of the tool. “Treebot” consists of a rack and pinion arrangement which uses mechanical springs to accomplish compression [20]. A variable stiffness spring is used in the Anterior Cruciate Ligament reconstruction steerable drill. It is controlled using cables but has a restrained bending curvature [21]. Another catheter styled robotic system merges the tendon based approach with a concentric tube design permitting extension as well as bending. However, the motion of the robot is only possible with a heavy servo apparatus based testbed [22].

Analyzing and evaluating the three main design strategies used until now for constructing existing continuum robots [2], and the results provided by “Tendril” study [23], a sketch for a novel design concept was implemented [5]. In Section II, this paper introduces and details the structure and implementation of a first prototype of this long and thin continuum cable robot and its noteworthy compact actuation mechanism. The unique focus on aspect ratio with respect to length and width (around 100:1) and the incorporation of convenient features of the concentric tube design in a spring-loaded tendon based design at this scale, to the best of our knowledge, is the first of its kind. The procedure for its modified kinematic modelling is specified in Section III. The results from the performance evaluation for this design and its kinematics are presented and discussed in Section IV. Future work and conclusion are presented in Sections V and VI.

II. DESIGN SPECIFICS OF THE ROBOTIC CABLE

A. Objectives for the Construction of Prototype

“Tendril” utilized springs to ensure a thin profile but ended up facing issues such as uncontrollable buckling of backbone elements, twisting of sections and inability to compress/extend locally [4]. Since pneumatics/hydraulics which provide contraction/extension easily is avoided due to sizing constraints, springs are considered essential for the same (non-fluidic) feature. The modified tentacle arm variant [9] developed earlier used tension springs to attain varied but limited section lengths. Drawing insight in our novel design, compression springs were theorized to be used in a similar fashion but combined with concentric tubes to remove the shortcoming of uncontrollable compression but still providing the needed feature of local contraction.

The robotic cable consists of three backbone elements arranged in a telescoping concentric fashion. Tendon driven springs along the backbone gives tunable impedance. This approach replaces the large linear actuation system normally required for concentric tube designs. Bending and compression/extension is given by the relative pulling of tendons against the compression springs.

Thus, the preferred design objectives for the robot are:

1. Clean and simple mechanical design.
2. Thin profile but relatively long length (1:100).
3. Controllable bending about the entire cable length.
4. Local compression and extension
5. Compact electrical actuator package.

B. Architecture of the First Long and Thin Prototype

The robotic cable is a 139 cm long tendon-based three section continuum arm. About 55% of its length is 0.7 cm in diameter and the remainder is 1.4 cm in diameter. All three sections use nitinol as the main backbone element. Nitinol is an alloy composed of nickel and titanium. Its super elasticity, high tensile strength, ready availability in various forms like wires, rods, tubes, etc., and in desired dimensions makes it an ideal material for slim but long continuum cables. Such nitinol tubes can be easily bent and coiled into a reel-like mechanism simplifying its storage, like the actuator package for “Tendril” [4]. The distal section is a rod while the middle and base sections are tubes. The dimensions of the three sections are so chosen that they can be arranged in a concentric telescoping fashion, with the distal rod sliding freely inside the middle tube and the middle tube in turn sliding freely in the base tube. The dimensions of the tubes are specified in Table I.

TABLE I. NITINOL BACKBONE DIMENSIONS

Robotic cable Section	Outer diameter (cm)	Inner diameter (cm)	Free length (cm)	Length inside next section (cm)
Distal	0.1	NA	34	15
Middle	0.17	0.13	45	7.5
Base	0.21	0.19	60	NA

Small plastic spacers, which are 3D printed, are used as the tendon guides. The material used for the plastic is PolyJet photopolymer. They are circular in profile with a central cavity to accommodate the nitinol backbone elements. Each has three tendon guide holes spaced at 120° along the

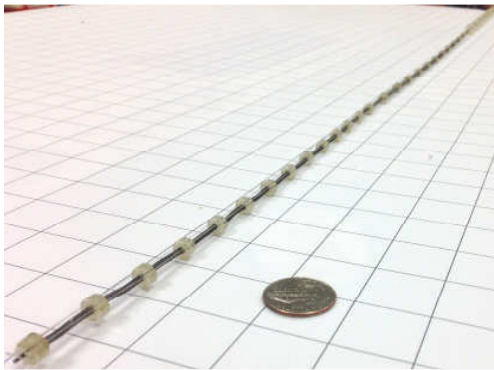


Figure 2. Robotic cable prototype (alongside a US quarter)

periphery of the spacer. The tendon guide hole set for each backbone element is thus spaced at 40° with respect to the adjacent section set. The dimensions of the spacers are specified in Table II.

A key novelty of this design is the use of compression springs to hold the above spacers in their place at a fixed

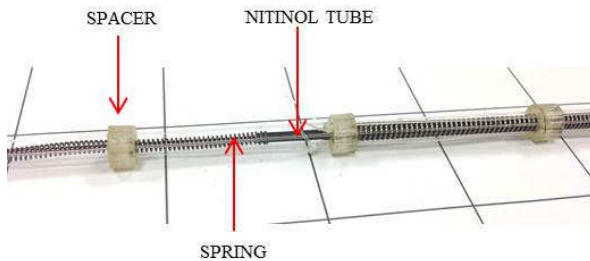


Figure 3. Spring supported concentric arrangement of continuum sections

TABLE II. SPACER DIMENSIONS

Robotic cable Spacers	Spacer diameter (cm)	Spacer width (cm)	Central cavity diameter (cm)	Tendon diameter (cm)
Distal	0.7	2.5	0.12	0.1
Middle	0.7		0.2	
Base	1.4		0.25	

distance and provide for the active local compression of their telescoping backbones as shown in Fig. 3. This translation is achieved using motor driven tendons, avoiding any additional or dedicated linear actuation mechanism. The material used for the springs is music wire. The spring parameters are as in Table III. In order to minimize coupling between sections, it was ensured that the springs for the middle section will have double the stiffness constant in comparison with the ones used for the distal section.

Nylon fishing lines of 0.07cm diameter serve as tendons for this cable robot.

TABLE III. SPRING PARAMETERS

Robotic cable Section	Outer diameter (cm)	Inner diameter (cm)	Spring rate (lb/in)	Length (cm)
Distal	0.224	0.163	2.3	2.54
Middle	0.3	0.213	4.15	3.81

C. Functioning of the Robotic Cable

The constructed robotic cable consists of three backbone elements which can be approximated as a series of constant curvature sections. The actuation caused by pulling on a specific tendon produces bending in the same plane and corresponding direction. The three tendons can effect bending in three dimensions i.e. 3 actuated DOF. Since the robotic cable comprises of three sections, it has 9 actuated DOF in total.

The springs are normally in a relaxed state. However, on pulling on all three tendons simultaneously, the concentric and telescoping arrangement of the tubes enable controlled translational motion of the sections relative to each other.

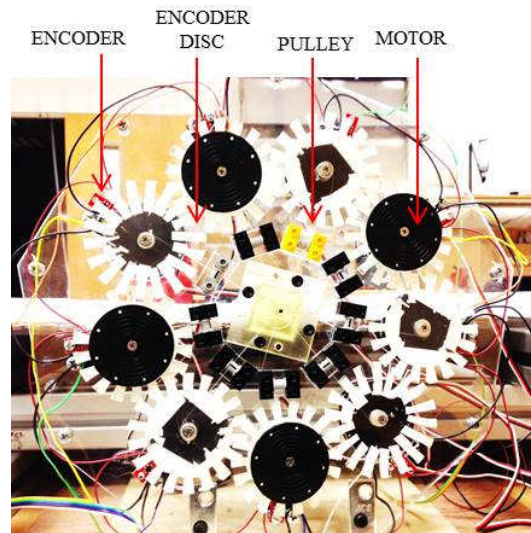


Figure 4. Actuation mechanism

In the case of retracting all three tendons of, say, the distal section, the springs on it will contract up to their base length, thus counteracting the force, and that backbone section will slide inside the middle tube. The coupling between the sections will cause the springs on the middle section to compress as well to some extent and that in turn will move inside the base section. When the tendons are relaxed, the springs will acquire their initial relaxed state and the sections will return to their positions as before. The springs thus support finite controllable translational motion. All this can be seen in the video attachment.

The actuator assembly consists of 9 RC servo motors spaced at 40° which are arranged on an acrylic base plate as shown in Fig. 4. Each of the 9 tendons is connected to individual servos via a pulley mechanism. Each servo is provided with an encoder sensor to provide position feedback. The servos are controlled using an Arduino microcontroller board.

The RC servos help to avoid the need for complex control schemes. They have high torque capacities which actuate the robotic cable effectively. They are easily controlled using the Arduinos. The encoders give pulses/counts corresponding to the motor shaft position enabling determination of the cable tip. The compact and simple design arrangement of the complete mechanism can be seen operating successfully in the video attachment.

III. KINEMATIC MODELLING

A. Determination of Length Change and Compression Variables for the Robotic Cable

The initial baseline modeling for the robotic cable is based on the forward kinematic formulas developed in [24].

Continuum sections which are approximated by a constant curvature use shape variables viz., λ , ϕ and θ as shown in Fig. 5. λ gives the radius of curvature, ϕ determines the elevation angle and θ gives the angle of the bending plane as a function of length changes $q_j = [l_{j1}, l_{j2}, l_{j3}]^T$ for each section (here $j = 1, 2, 3$) with respect to the unactuated original L_0 for each section. r_j is the distance from the center

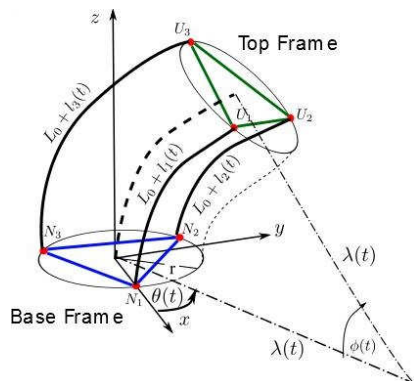


Figure 5. Continuum section schematic and geometrical variables [15]

of the manipulator to the location of the tendons. The forward kinematics equations derived in [24] can be implemented as shown below for each section.

$$\lambda_j(q_j) = \frac{(3L_{j0} + l_{j1} + l_{j2} + l_{j3})r_j}{2\sqrt{l_{j1}^2 + l_{j2}^2 + l_{j3}^2 - l_{j1}l_{j2} - l_{j1}l_{j3} - l_{j2}l_{j3}}} \quad (1)$$

$$\phi_j(q_j) = \frac{2\sqrt{l_{j1}^2 + l_{j2}^2 + l_{j3}^2 - l_{j1}l_{j2} - l_{j1}l_{j3} - l_{j2}l_{j3}}}{3r_j} \quad (2)$$

$$\theta_j(q_j) = \tan^{-1} \left\{ \frac{\sqrt{3}(l_{j3} - l_{j2})}{l_{j2} + l_{j3} - 2l_{j1}} \right\} \quad (3)$$

The arc length s can then be computed as $s_j = \lambda_j \phi_j$.

$$s_j = \frac{3(L_{j0}) + l_{j1} + l_{j2} + l_{j3}}{3} \quad (4)$$

The above formulation, however, cannot be applied directly to the continuum robotic cable due to the added unique feature of actively controllable contraction in its middle and distal sections, which is coupled with its bending. In order to incorporate this compression in the modeling, experiments were performed to establish a relationship between the actual lengths of the tendons being pulled to achieve bending or compression and the effective lengths being pulled given the known spring stiffness.

To reduce the effect of gravity, the cable was placed on a table to analyze the 2D planar performance (therefore only l_{j1} and l_{j2} will be considered) of its middle section and distal sections as shown in Fig. 2, since these are the sections having springs in their design and compression has to be taken into account in the kinematics. Let l_{ji} ($i = 1, 2, 3$) indicate the length changes q_j . One experiment was to study the robot's active bending capabilities. The change in length q_j in every case, however, is not with respect to the initial length L_{j0} but with the modified initial length $(L_{j0} + c_j)$ where $c_j \in \mathbb{R}_0^-$ is compression (due to the

TABLE IV. EXPERIMENTAL DATA FOR DISTAL SECTION (AVERAGE VALUES)

Encoder counts σ	Angle (rad) ϕ	Radius (cm) λ	Arc length (cm) $s = \lambda\phi$
0	0	Inf	34
14	0.4794	69.89	33.52
31	0.6365	51.76	32.95
57	0.9070	35.6	32.29
81	1.0948	28.05	30.71
107	1.3175	22.46	29.59
145	1.5167	18.612	28.23

springs) in addition to the length changes q_j which accounts for the coupling. A mapping was established by relating the encoder pulse counts corresponding to given curvature of the distal arm and the associated change in the length of the tendon actuated. The range of encoder counts was a choice based on the bending capability (of the section under consideration). Table IV shows the experimental data.

The above data is obtained by actuating tendon 1 (i.e. length change is l_{31}) for the distal section. Hence (2) simplifies to (5). Knowing r_3 and ϕ_3 from the experimental data, l_{31} can be computed.

$$\phi_3(q_3) = \frac{2l_{31}}{3r_3} \quad (5)$$

The data obtained from the experiments suggested that line fit approximations could be used to establish the counts and length change relationship since the spring is linear. Also, there is no length change l_i when the encoder count σ_i is zero. The linear model relating length changes and encoder counts hence given by,

$$l_{3i} = m_3 \sigma_{3i} \quad (6)$$

On repeating the experiment several times the slope constant average m_3 was computed to be $m_3 = -3.648 \times 10^{-5}$ (m). Knowing L_{30} , s_3 from the experimental data and l_{31} computed above, the compression c_{31} can be estimated from the modified (4) given below,

$$s_3 = \frac{3(L_{30} + c_{31}) + l_{31}}{3} \quad (7)$$

The coupled compression c_{31} was then found as a linear function of encoder counts using slope constant average n_3 ,

$$c_{3i} = n_3 \sigma_{3i} \quad (8)$$

After multiple tests, the slope constant n_3 was computed to

TABLE V. EXPERIMENTAL DATA FOR MIDDLE SECTION (AVERAGE VALUES)

Encoder counts σ	Angle (rad) ϕ	Radius (cm) λ	Arc length (cm) $s = \lambda\phi$
0	0	Inf	45
37	0.17	260.64	44.31
55	0.2754	158.43	43.63
91	0.3752	113.89	42.73
118	0.475	88.9	42.25
126	0.5365	78.28	41.99
151	0.6032	68.67	41.42

be $n_3 = -4.12 \times 10^{-4}$ (m). When all three tendons are pulled simultaneously, pure compression motion is achieved.

The above procedure was repeated for the middle section as well. Table V shows the experimental data shown below is obtained by actuating tendon 1.

After several experiments, the slope constant averages m_2 and n_2 were determined to be $m_2 = -1.329 \times 10^{-5}$ (m) and $n_2 = -2.36 \times 10^{-4}$ (m).

Using these derived changes in lengths and coupled compressions as a function of encoder counts in the forward kinematic equations (1) to (3), the performance of the robotic cable can be predicted. The unactuated original length L_{j0} is now augmented with additional compression values c_{ji} for the middle and distal sections. The modified formulations, using (6) and (8) for describing the shape configuration of the continuum cable is as expressed in (9), (10) and (11).

$$\lambda_j(\sigma_{ji}) = \frac{(3(L_{j0} + n_j \sum_{i=1}^3 \sigma_{ji}) + m_j \sum_{i=1}^3 \sigma_{ji})r_j}{2m_j \sqrt{\sigma_{j1}^2 + \sigma_{j2}^2 + \sigma_{j3}^2 - \sigma_{j1}\sigma_{j2} - \sigma_{j1}\sigma_{j3} - \sigma_{j2}\sigma_{j3}}} \quad (9)$$

$$\phi_j(\sigma_{ji}) = \frac{2m_j \sqrt{\sigma_{j1}^2 + \sigma_{j2}^2 + \sigma_{j3}^2 - \sigma_{j1}\sigma_{j2} - \sigma_{j1}\sigma_{j3} - \sigma_{j2}\sigma_{j3}}}{3r_j} \quad (10)$$

Since the robot is analyzed in a planar orientation herein, the angle of bending plane θ is zero. In general, it will be given as,

$$\theta_j(\sigma_{ji}) = \tan^{-1} \left\{ \frac{\sqrt{3}(\sigma_{j3} - \sigma_{j2})}{\sigma_{j2} + \sigma_{j3} - 2\sigma_{j1}} \right\} \quad (11)$$

B. Direct Kinematic Modeling

The homogenous transformation matrix (HTM) for a j^{th} section [24] will now use the shape variables derived in equations (9) and (10) as function of the encoder counts.

$$T_j = \begin{bmatrix} \cos(\phi_j(\sigma_{ji})) & \sin(\phi_j(\sigma_{ji})) & 0 & \lambda_j(\sigma_{ji})(1 - \cos(\phi_j(\sigma_{ji}))) \\ -\sin(\phi_j(\sigma_{ji})) & \cos(\phi_j(\sigma_{ji})) & 0 & \lambda_j(\sigma_{ji})\sin(\phi_j(\sigma_{ji})) \\ 0 & 0 & 1 & 0 \\ 0 & 0 & 0 & 1 \end{bmatrix} \quad (12)$$

Considering that the robotic cable is a 3 section continuum arm, the complete HTM will be given as,

$${}^0_3T = {}^0_1T \cdot {}^1_2T \cdot {}^2_3T \quad (13)$$

Since there are no springs in the base section, can be computed using the direct kinematic formulas as in (1), (2)

and (3). However, it is still necessary to relate its shape variables to measurable variables. The method is the same as described for the middle and distal sections, except that compression term is absent and only the linear relationship between length changes and the encoder counts needs to be used for computation of 0_1T

This completes the forward kinematic model for the long and slim continuum robotic cable.

IV. RESULTS AND DISCUSSION

The modified direct kinematic equations derived in Section III were implemented in MATLAB® providing the encoder counts as inputs and computing the various shape variables of the robot to consider the effect of the new design of the robot on its performance. These variables were then fed into the direct kinematic model to get the position variables of the cable.

The *xy*-coordinate indicating the position of the tip of the robotic cable was computed, considering the cable as a single section continuum arm consisting of the middle section alone.

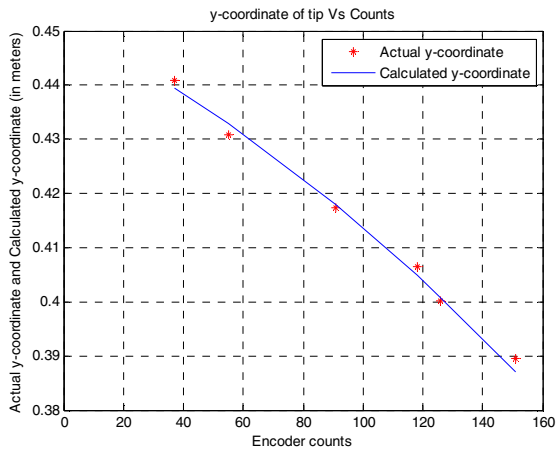


Figure 6. Y-coordinate of middle section tip relative to encoder counts

Fig. 6-7 show the output given by the kinematic model on inputting the calculated shape variables value in comparison with the actual values obtained from the experimental data. The results agree quite well. It implies that the linear approximations incorporated in the modeling to account for the effect of the springs-loaded tendon design is justified. Also, the middle section is less compressible as compared to the distal section and there is absence of compressive coupling with the base section (which lacks springs). The tendon is also oriented in the horizontal plane where bending is actually intended. All this helps the direct transfer of the total forces to achieve bending.

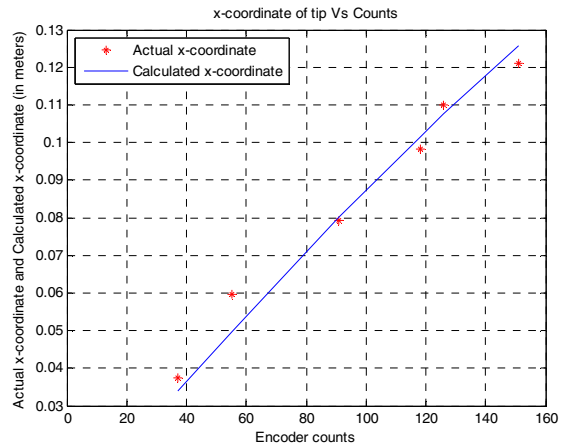


Figure 7. X-coordinate of middle section tip relative to encoder counts

The same procedure was repeated for the distal section. Fig. 8-9 depicts the comparative results.

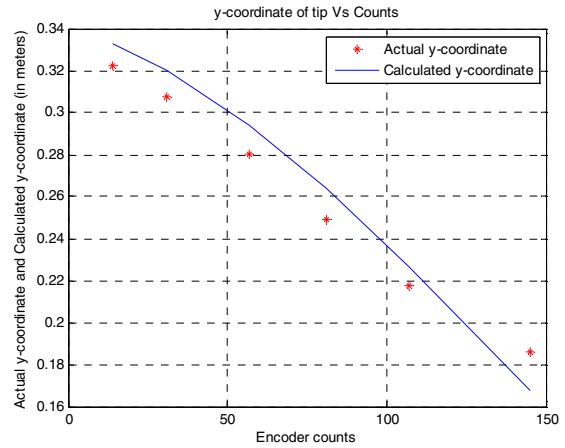


Figure 8. Y-coordinate of the distal section tip relative to encoder counts

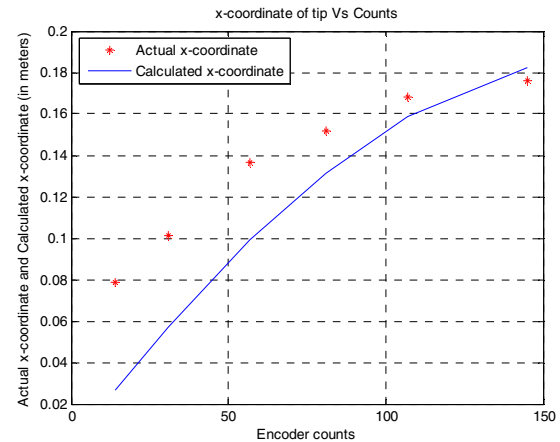


Figure 9. X-coordinate of distal section tip relative to encoder counts

The results are reasonable for the y-coordinate of the tip position. For the x-coordinate, however, the results are not that satisfactory. The main reason for this may be attributed to certain unmodeled effects. One major factor is the inherent friction present on the 2D experimental surface. Also, the robot is designed for operation in 3D space but is arranged in a planar manner. Thus, due to the orientation of tendons (120° apart), only a component of the force actuating the tendon intended to cause bending, deflects it in the horizontal plane in this section. The tendon tries to deflect in a plane angular to the horizontal surface, thereby thrusting the section on the surface. This results in more frictional forces. This will, however, not be the case in 3D space. Thus, friction and tendon orientation affects the results obtained significantly. Another factor can be the unmodeled effects of the motor and sensor systems.

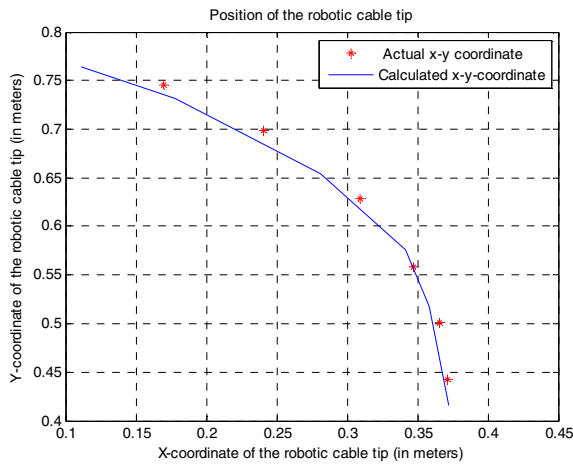


Figure 10. Position of the end point of the robotic cable

Finally, the robotic cable was operated as a two section continuum manipulator (middle and distal sections since those incorporated the spring-loaded concentric tube aspect of the design) and the 2D HTM for the multi-section version, as a function of the encoder inputs, as in (13), was computed. The resulting position of the end of the robotic cable provided by the kinematic model was plotted in comparison with the actual position. Fig. 10 shows excellent results for this two section version of the cable. Thus, linear regression method is quite effective in the kinematic modeling of such multi-section long and slim continuum robotic cable having local compressibility feature using spring driven tubular backbone elements.

V. CONCLUSION AND FUTURE WORK

We have presented and analyzed the first actuated prototype of a new type of long and thin continuum robotic cable. Based on a spring-loaded continuum tube design, the robot is actuated entirely via tendons. This allows a significantly smaller actuator package than for previous

concentric tube designs, which required linear actuation at the robot base. The long thin design of the cable robot features actuation of both bending and local extension/contraction. We present a kinematic analysis of the design, supported by experiments with the prototype. Modifications of established continuum robot kinematics to take into account the effect of spring loading are seen to be effective.

The work proposed in this paper is in an ongoing phase. In future, an actuator unit consisting of a coiling mechanism on the lines of the “Tendrill” housing [4] will be constructed. A suitable soft covering sheath will be provided to enclose the entire length of cable and thereby protect the tendons, spacers and the nitinol backbone from inadvertent damage. A camera will be attached at the end of the robot to have visual feedback for potential inspection applications. The three sections will be further modeled to consider the relative arrangement (40° spacing) of tendons in the adjacent sections in 3D operations. The effect of torsion and dynamic models can also be integrated. Ultimately, the robotic cables performance in a real life 3D environment will be evaluated using model based control algorithms.

ACKNOWLEDGMENT

This research was supported in part by NASA under contract NNX12AM01G, and in part by the U.S. National Science Foundation under grant IIS-0904116.

REFERENCES

- [1] G. Robinson and J. B. C. Davies, “Continuum Robots - A State of the Art,” Proceedings IEEE International Conference on Robotics and Automation, Detroit, Michigan, pp. 2849-2854, 1999.
- [2] I. D. Walker, “Robot strings: long, thin continuum robots,” in Proceedings of the IEEE Aerospace Conference, pp. 1-12, Big Sky, Mont, USA, 2013.
- [3] P. Dupont, J. Lock, B. Itkowitz, and E. Butler, “Design and control of concentric tube robots,” IEEE Trans. Robot., vol. 26, no. 2, pp. 209-225, Apr. 2010.
- [4] J.S. Mehling, M.A. Diftler, M. Chu, and M. Valvo, “A Minimally Invasive Tendril Robot for In-Space Inspection”, Proceedings BioRobotics 2006 Conference, pp 690-695, 2006.
- [5] M.M. Tonapi, I.S. Godage, I.D. Walker, “Next-Generation Rope like Robot for In-Space Inspection” in IEEE Aerospace Conference proceedings, Big Sky Montana, USA, March 2014.
- [6] J. Yang, P. Jason, K. Abdel-Malek. “A Hyper-Redundant Continuous Robot” in IEEE International Conference on Robotics and Automation, 2006.
- [7] K. Hatazaki, M. Konyo, S. Tadokoro, “Active Scope Camera for Urban Search and Rescue”, Proc. 2007 IEEE/RSJ International Conference on Intelligent Robots and Systems (IROS2007), pp.2596-2602, 2007.
- [8] I. Gravagne, C. Rahn, and I. D. Walker, “Large Deflection Dynamics and Control for Planar Continuum Robots,” IEEE/ASME Transactions on Mechatronics, vol. 8, no. 2, pp. 299-307, June 2003.
- [9] M. Blessing and I.D. Walker, “Novel Continuum Robots with Variable-Length Sections”, 3rd IFAC Symposium on Mechatronics Systems, Sydney, Australia, September 2004
- [10] A. Kapoor, N. Simaan and R.H. Taylor, “Suturing in confined spaces: Constrained motion control of a hybrid 8-dof robot”, ICAR. (2005) 452-459.
- [11] A. Degani, H. Choset, A. Wolf, and M. Zenati, “Highly articulated robotic probe for minimally invasive surgery,” in Proc. IEEE Int. Conf. Robot. Autom., Orlando, FL, 2006, pp. 4167-4172.

- [12] T.D.Maahs, V.Saadat, C.Rothe and T.T.Le, "Disposable shapelocking system" Patent number US 20060058582 A1.
- [13] Y. Chen, et al, "Multi-turn, Tension-stiffening Catheter Navigation System," 2010 IEEE ICRA, Anchorage, AK, 2010.
- [14] Webster, R. J., III, Romano, J. M. and Cowan, N. J. (2009). Mechanics of precurved-tube continuum robots. *IEEE Transactions on Robotics*, 25(1): 67–78.
- [15] I. S. Godage, D. T. Branson, E. Guglielmino, G. A. Medrano-Cerda, and D. G. Caldwell, "Shape Function-Based Kinematics and Dynamics For Variable Length Continuum Robotic Arms," in *IEEE International Conference on Robotics and Automation*, 2011.
- [16] I. S. Godage, D. T. Branson, E. Guglielmino, G. A. Medrano-Cerda, and D. G. Caldwell, "Dynamics for Biomimetic Continuum Arms: A Modal Approach," in *IEEE Int. Conf. on Robotics and Biomimetics*, 2011, pp. 104–109.
- [17] Y. Chen, S. Tanaka, and I. W. Hunter, "Disposable endoscope tip actuation and robotic platform," in *32nd Annual International Conference of the IEEE Engineering in Medicine and Biology Society*, pp. 2279–2282, 2010.
- [18] M. Mahvash and M. Zenati, "Toward a Hybrid Snake Robot for Single-Port Surgery" *IEEE EMBS Boston, Massachusetts USA, August 30 -September 3, 2011*.
- [19] C. A. Velasquez, H. H. King, B. Hannaford, and W. J. Yoon, "Development of a flexible imaging probe integrated to a surgical telerobot system: Preliminary remote control test and probe design," in *Proc. IEEE RAS EMBS Int. Conf. Biomedical Robotics and Biomechatronics, Rome, Italy, 2012*, pp. 894–898.
- [20] T.L. Lam, Y.S.Xu (2012) Biologically inspired treeclimbing robot with continuum maneuvering mechanism, *Journal of Field Robotics*, 29(6), 843–860.
- [21] H. Watanabe, K. Kanou, Y. Kobayashi, and M. G. Fujie, "Development of a "steerable drill" for ACL reconstruction to create the arbitrary trajectory of a bone tunnel," in *Proceedings of the IEEE/RSJ International Conference on Intelligent Robots and Systems: Celebrating 50 Years of Robotics (IROS '11)*, pp. 955–960, San Francisco, Calif, USA, September 2011.
- [22] J. Jung, R.S. Penning, M.R. Zinn and N.J.Ferrier, "A Modeling Approach for Continuum Robotic Manipulators: Effects of Nonlinear Internal Device Friction," *Intelligent Robots and Systems*, 2011 *IEEE International Conference*.
- [23] L. Cowan, *Analysis and Experiments for Tendril-Type Robots*, M.S. Thesis, Clemson University, May 2008.
- [24] I.S. Godage, E. Guglielmino, D.T. Branson, G.A.Medrano-Cerda, and D.G. Caldwell, "Novel Modal Approach for Kinematics of Multisection Continuum Arms", *Proceedings IEEE/RSJ International Conference on Intelligent Robots and Systems, San Francisco, CA*, pp 1093-1098, 2011.